

Supporting Information

Inert Gas Condensation made bimetallic FeCu nanoparticles - plasmonic response and magnetic ordering

Kamila Kollbek, Piotr Jabłoński, Marcin Perzanowski, Dominika Święch, Marcin Sikora, Grzegorz Słowik, Mateusz Marzec, Marta Gajewska, Czesława Paluszakiewicz and Marek Przybylski

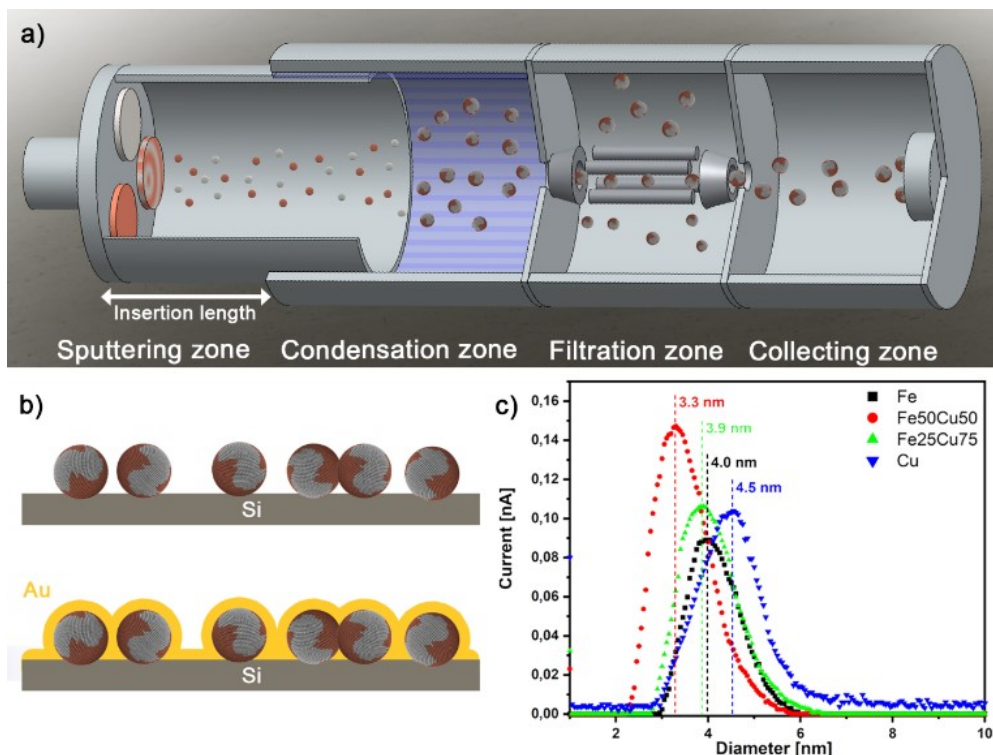


Figure S1 Schematic view of a) the vacuum deposition system based on IGC technique containing the NPs source (Mantis Deposition Ltd), b) two type of deposited systems: NPs without (top) and with 3 nm thick film of Au (bottom). c) Distribution of the electrical current carried by Cu, Fe and bimetallic FeCu NPs collected at the exit grid of the quadruple mass spectrometer as a function of the diameter of the selected mass of NPs. The frequency of the quadruple mass spectrometer at which the electrical current reaches a maximum (given by dashed vertical line) was chosen as a desire NPs diameter.

Table S1 Deposition parameters for studied NPs.

Sample	Working pressure [mTorr]	Input current [mA]	Argon flow [sccm]	Insertion length [mm]	Time [min]
Fe	4.7	70	70	10	40
Fe50Cu50	5.1	100	100	0	40
Fe25Cu75	5.0	100	100	0	40
Cu	60.0	110	100	30	40

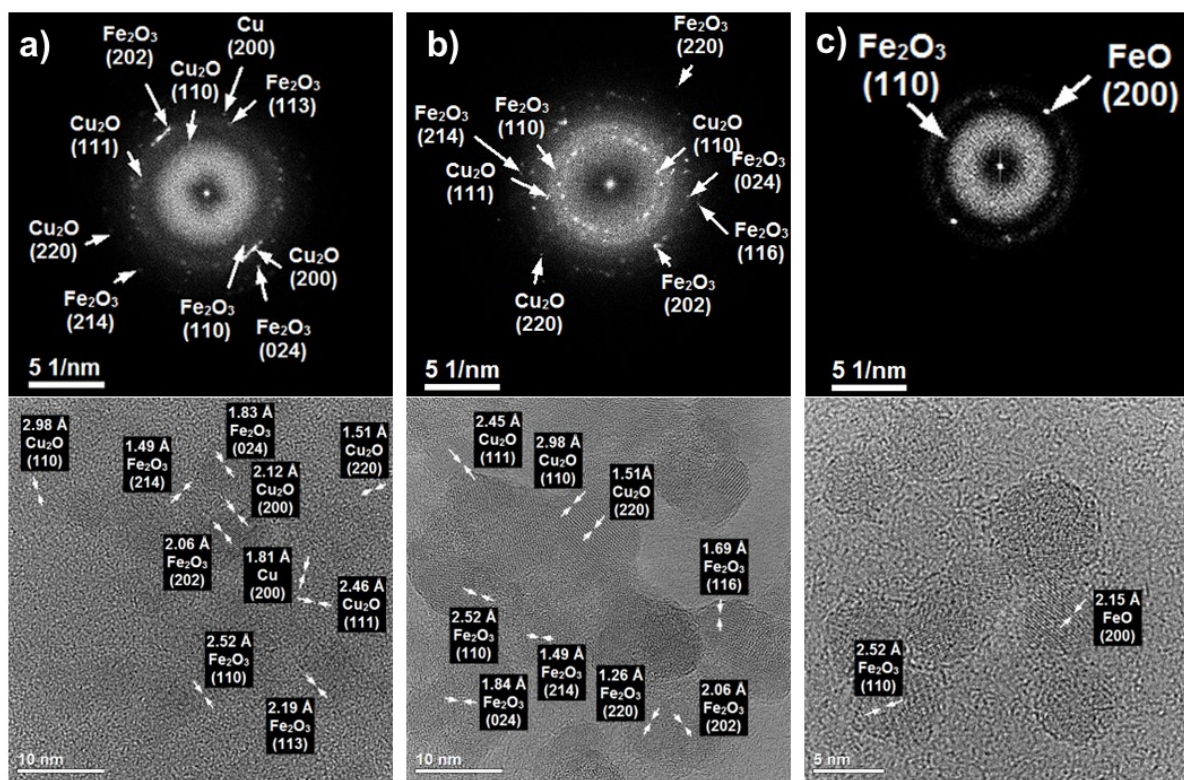


Figure S2 HR-TEM image of the iron, cooper and bimetallic a) Fe50Cu50 b) Fe25Cu75, c) Fe NPs with the proposed lattice planes of the detected structural phases together with the electron diffraction pattern.

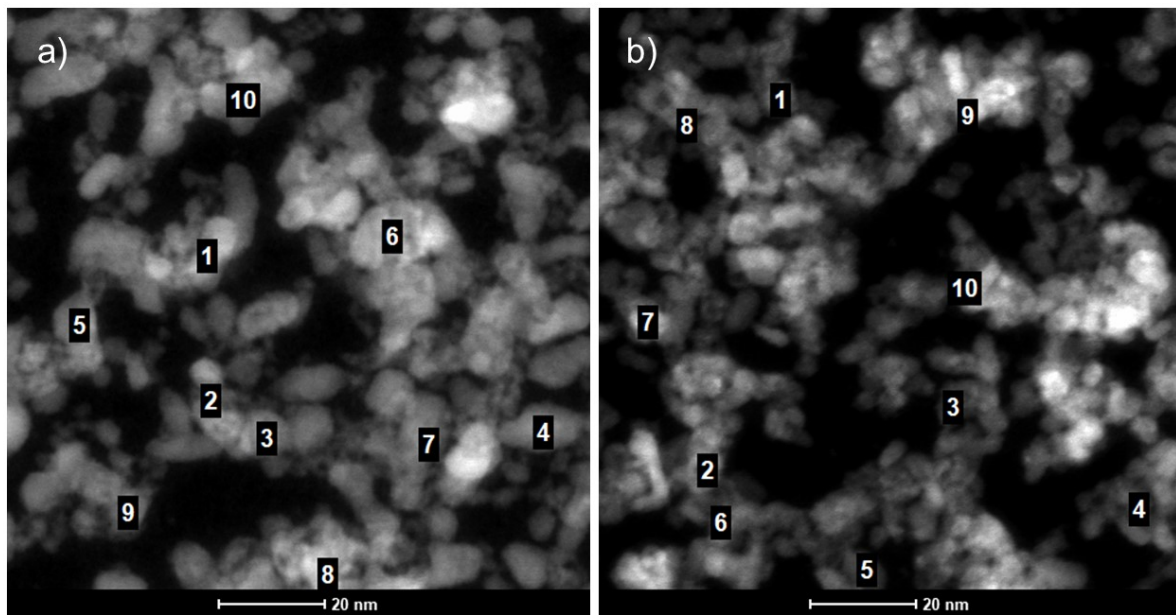


Figure S3 SEM image with marked 10 nanoparticles for which EDS analysis was performed for a) Fe25Cu75 and b) Fe50Cu50 NPs.

Table S2 The atomic% content of Cu and Fe in the studied bimetallic samples of Fe25Cu75, Fe50Cu50 NPs based on the EDS method for 10 selected nanoparticles.

Fe25Cu75			Fe50Cu50		
No	Cu (atomic %)	Fe (atomic %)	No	Cu (atomic %)	Fe (atomic %)
1	74.8	25.2	1	55.6	44.4
2	68.4	31.6	2	50.4	49.6
3	76.3	23.7	3	46.1	53.9
4	80.5	19.5	4	49.2	50.8
5	76.8	23.2	5	56.7	43.3
6	73.4	26.6	6	58.7	41.3
7	76.7	23.3	7	45.7	54.3
8	76.6	23.4	8	41.3	58.7
9	77.9	22.1	9	56.4	43.6
10	77.7	22.3	10	56.3	43.7
Average	75.9±3.2	24.1±3.2	Average	51.6±5.9	48.4±5.9

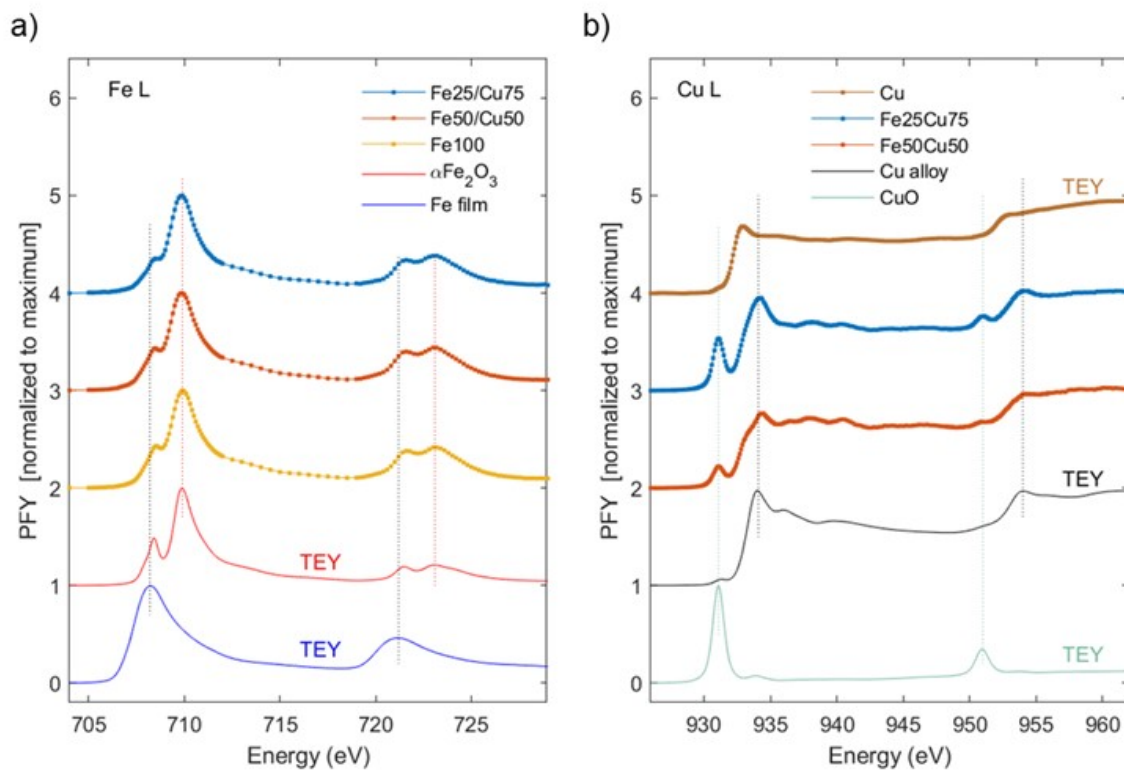


Figure S4 PFY XAS at Fe and Cu L absorption edges. Chemical and structural characteristics of FeCu NPs can be deduced by comparison with spectra of reference samples, namely iron(III) oxide and metallic film as well as copper(II) oxide and CuO.

Table S3. Wavenumbers and proposed band assignment for the Raman, FT-IR, SERS and SEIRA spectra of Phe adsorbed onto Cu, Fe25Cu75, and Fe50Cu50 NPs.

Assignment	Wavenumber [cm ⁻¹]							
	Phe Raman	FT-IR	Cu SERS	SEIRA	Fe25Cu75 SERS	SEIRA	Fe50Cu50 SERS	SEIRA
v(NH)	3169							
v(NH)		3125		3120				
v ₂ , v(CH) _{ring}	3065	3060	3061	3061	3059		3061	3030
v(CH)	3040	3028	3034	3030	3039	3030		3030
v _{as} (CH)	2967		2962				2967	
v _{as} (CH)	2927	2918	2925		2938	2918	2923	2922
v _s (CH)	2858		2867		2870		2860	
ρ _{bas} (NH)		1634						
v _{8a} v(CC) _{ring} i. p.	1600	1609	1604	1605	1604	1603	1601	1604
v _{as} (COO); v _{8b} v(CC) _{ring}	1583	1589	1583	1585	1583	1579	1585	1580
v _{19a} v(CC) _{ring} ; ρ _{bs} (NH)		1503		1497		1518		1518
v _{19b} v(CC) _{ring} ; ρ _s (CH ₂)	1445	1448	1439	1455	1451	1456	1438	1457
v _s (COO)	1408	1408		1402		1398		1399
v ₃	1340	1366		1365		1345		
δ(CO)	1306	1325	1318	1322	1324	1314	1312	1313
v _{7a}	1212	1210	1209	1208	1206		1212	1207

ν_{9a}	1182	1197	1177	1195	1182	1162
δ (CH)		1143				
ν (CN)		1074		1073	1073	1074
ν_{18a} , i. p.	1035	1028	1029	1028	1031	1032
ν_{12}	1002		1001		1000	1002
ν (COO)	912					
$\delta_{o.o.p.}$ (C-H) _{ring}	850					
ρr (CH ₂)	832		822		810	824
δ (ring)			773		773	
ν_{11} , $\delta_{o.o.p.}$ (C-H) _{ring}	745		745		746	744
ρ_r (COO)	682		672		667	668
ν_{6b}	619		619		619	620
Abbreviations:	ν – stretching, δ – deformation, ρb – bending, ρr – rocking, ρs – scissoring, i.p. – in-plane, o.o.p. – out-of-plane, s – symmetric, and as – asymmetric vibrations;					